Passivity-Based Trajectory Control of an Overhead Crane by Interconnection and Damping Assignment

Harald Aschemann

Abstract This paper presents a passivity-based control scheme for the two main axes of a 5 t-overhead crane, which guarantees both tracking of desired trajectories for the crane load and an active damping of crane load oscillations. The passivity-based control is performed by interconnection and damping assignment according to the IDA-PBC approach for underactuated systems. The tracking capabilities concerning desired trajectories for the crane load can be significantly improved by introducing feedforward control based on an inverse system model. Furthermore, a reduced-order disturbance observer is utilised for the compensation of nonlinear friction forces. In this paper, feedforward and feedback control as well as observer based disturbance compensation are adapted to the varying system parameters rope length as well as load mass by gain-scheduling techniques. Thereby, desired trajectories for the crane load position in the 3-dimensional workspace can be tracked independently with high accuracy. Experimental results of an implementation on a 5 t-crane show both excellent tracking performance with maximum tracking errors of 2 cm and a high steady-state accuracy.

1 Introduction

In the last decade, numerous model-based trajectory control schemes for overhead travelling cranes have been proposed by different authors. Besides non-linear control approaches exploiting differential flatness [2], gain-scheduling techniques have proved efficient [1, 5]. Aiming at an increased handling frequency and a fully automated crane operation, the focus has to be on the motion of the crane load. Feedback control provides for tracking of desired trajectories for the crane in the 3-dimensional workspace with small tracking errors. In practical implementations,

Harald Aschemann
Chair of Mechatronics, University of Rostock, D-18059 Rostock, Germany;
E-mail: harald.aschemann@uni-rostock.de

H. Ulbrich and L. Ginzinger (eds.), Motion and Vibration Control, 21–30.

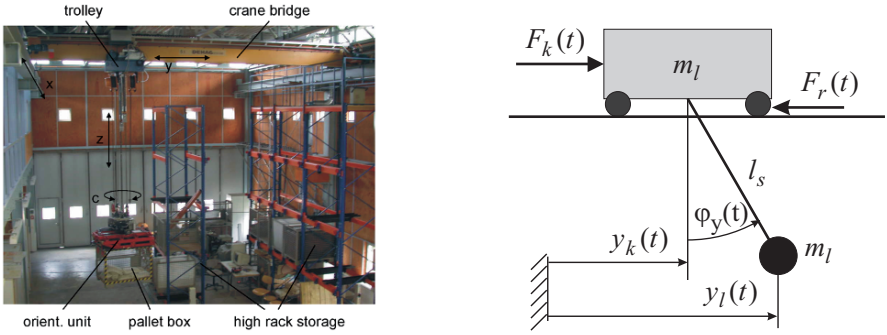

Fig. 1 Structure of the overhead travelling crane (left), Mechanical model of the y-axis (right).

however, tracking accuracy as well as steady-state accuracy strongly depend on the inclusion of appropriate control action to counteract disturbances, especially nonlinear friction acting on the drives as the dominant disturbance. Furthermore, a robust or adaptive control approach is necessary as regards varying system parameters like rope length or load mass during crane operation [5]. By this, the capabilities of an automated overhead crane can be extended in order to use it as a robot manipulator for the handling of heavy loads in a large cartesian workspace.

In this paper, the first principle modelling of the two main translational crane axes is addressed first. Aiming at a decentralised control structure, for each axis a separate design model is derived in symbolic form. Then, a state space model is established for the envisaged passivity-based control following the IDA-PBC approach for underactuated systems [3, 4, 6, 7]. The control design for the y-axis involves the control of the corresponding crane load position in y-direction, whereas the multi-variable control of the x-axis deals with both the crane load position in x-direction and the position difference of the two bridge drives, corresponding to a skew of the crane bridge. Feedforward control based on an inverse system model and friction compensation using disturbance observer have proved efficient to further reduce tracking errors. Thereby, desired trajectories for the crane load position in the xz-plane can be tracked independently with high accuracy. Experimental results of the closed-loop system show both excellent tracking performance and steady-state accuracy.

2 Modelling of the Crane y-Axis

As a decentralised control structure is envisaged, a separate design model of is used for each crane axis. Here, the modelling shall be presented only for the y-axis. The origin of the y-axis, $y_k = 0$, is located in the middle of the bridge. With a bridge length $l_{br} = 8.7$ m the available workspace in y-direction is characterised by $y_k \in [-4.35\,\text{m}, 4.35\,\text{m}]$. The crane axis is modelled as a multibody system with two

rigid bodies as shown in Figure 1. The trolley is modelled by a mass m_k, whereas the crane load is represented by a lumped mass m_l. The trolley is electrically driven by a motor force F_k. As the main disturbance nonlinear friction and damping are taken into account by the disturbance force F_r. This disturbance force is neglected at feedback control design but counteracted by both feedforward and observer-based disturbance compensation. The rope suspension is considered as massless connection, where rope deflections and small external damping are neglected. The two degrees of freedom for the mechanical model of the y-axis are chosen as the trolley position $q_1 = y_k$ and as the rope angle $q_2 = \varphi_y$. Then, the vector of generalized coordinates becomes $\underline{q} = [q_1, q_2]^T$. The rope length l_s is considered as a slowly varying system parameter and taken into account at control design by gain-scheduling techniques. By exploiting Langrange's equations, the equations of motion of the crane axis can be calculated and stated in the following matrix notation:

$$\underbrace{\begin{bmatrix} m_l + m_k & m_l\, l_s \cos(q_2) \\ m_l\, l_s \cos(q_2) & m_l\, {l_s}^2 \end{bmatrix}}_{\underline{M}} \ddot{\underline{q}} + \begin{bmatrix} -m_l\, l_s\, \dot{q}_2^2\, \sin(q_2) \\ m_l\, g\, l_s\, \sin(q_2) \end{bmatrix} = \underbrace{\begin{bmatrix} 1 \\ 0 \end{bmatrix} F_k}_{\underline{G}\, u} \tag{1}$$

3 Passivity-Based Control of Underactuated Systems

The open-loop underactuated system is governed by the Hamiltonian as the sum of kinetic and potential energy:

$$H(\underline{q}, \underline{p}) = \frac{1}{2} \underline{p}^T \underline{M}^{-1}(\underline{q})\, \underline{p} + V(\underline{q}) \tag{2}$$

At this, the generalised coordinates $\underline{q} \in \mathbb{R}^n$ and the generalised momentum $\underline{p} \in \mathbb{R}^n$ are used. With the symmetric, positive definite mass matrix $\underline{M}(\underline{q}) = \underline{M}^T(\underline{q}) > 0$ and the potential energy $V(\underline{q})$, the total energy of the underactuated system can be stated. As the friction as well as the damping forces are counteracted by an observer-based disturbance compensation, the passivity-based control design is based on the following state equations:

$$\begin{bmatrix} \dot{\underline{q}} \\ \dot{\underline{p}} \end{bmatrix} = \begin{bmatrix} \underline{0} & \underline{I} \\ -\underline{I} & \underline{0} \end{bmatrix} \begin{bmatrix} \nabla_{\underline{q}} H \\ \nabla_{\underline{p}} H \end{bmatrix} + \begin{bmatrix} \underline{0} \\ \underline{G}(\underline{q}) \end{bmatrix} \underline{u} \tag{3}$$

The matrix $\underline{G} \in \mathbb{R}^{n \times m}$ determines how the control input $\underline{u} \in \mathbb{R}^m$ acts on the system. For a fully actuated system $m = n$ holds, whereas for the crane as underactuated system $rank\,(\underline{G}) = m < n$ is given. The passivity-based control involves the design of a desired closed-loop Hamiltonian H_d

$$H_d(\underline{q}, \underline{p}) = \frac{1}{2} \underline{p}^T \underline{M}_d^{-1}(\underline{q}) \underline{p} + V_d(\underline{q}) \tag{4}$$

The matrix $\underline{M}_d = \underline{M}_d^T > 0$ denotes the mass matrix according to the desired kinetic energy and V_d the desired closed-loop potential energy. This energy function V_d to be determined must have a global minimum in the desired equilibrium $\underline{q}^*$. This leads to $\min V_d(\underline{q}) = V_d(\underline{q}^*)$. The control design (IDA – PC) can be divided into the following two steps:

1. Energy shifting by the control action $\underline{u}_{ev}(\underline{q}, \underline{p})$
2. Damping injection by the control action $\underline{u}_{di}(\underline{q}, \underline{p})$

The resulting control law is given by the sum of both control parts, i.e. $\underline{u} = \underline{u}_{ev} + \underline{u}_{di}$. For the calculation of the feedback control law, the following condition must hold for the closed-loop:

$$\begin{bmatrix} \dot{\underline{q}} \\ \dot{\underline{p}} \end{bmatrix} = \left(\underline{J}_d(\underline{q},\underline{p}) - \underline{R}_d(\underline{q},\underline{p})\right) \begin{bmatrix} \nabla_{\underline{q}} H_d \\ \nabla_{\underline{p}} H_d \end{bmatrix}$$

with the terms

$$\underline{J}_d = -\underline{J}_d^T = \begin{bmatrix} \underline{0} & \underline{M}^{-1}\,\underline{M}_d \\ -\underline{M}_d\,\underline{M}^{-1} & \underline{J}_z(\underline{q},\underline{p}) \end{bmatrix},\ \underline{R}_d = \underline{R}_d^T = \begin{bmatrix} \underline{0} & \underline{0} \\ \underline{0} & \underline{G}\,\underline{K}_d\,\underline{G}^T \end{bmatrix} > 0 \tag{5}$$

The matrix $\underline{J}_d$ describes the desired interconnection and $\underline{R}_d$ the damping matrix. The interconnection matrix $\underline{J}_d$ is extended by an additional interconnection part $\underline{J}_z$. The damping matrix $\underline{R}_d$ is introduced to provide sufficient damping in the closed-loop system. This is achieved be a negative feedback of the corresponding passive output, in the given case $\underline{G}^T \nabla_{\underline{p}} H_d$. As a result, the damping control action can be stated as

$$\underline{u}_{di} = -\underline{K}_d\,\underline{G}^T \nabla_{\underline{p}} H_d, \tag{6}$$

with the constant gain matrix $\underline{K}_d = \underline{K}_d^T$. The energy shifting control part $\underline{u}_{ev}$ is determined from

$$\begin{bmatrix} \underline{0} & \underline{I} \\ -\underline{I} & \underline{0} \end{bmatrix} \begin{bmatrix} \nabla_{\underline{q}} H \\ \nabla_{\underline{p}} H \end{bmatrix} + \begin{bmatrix} \underline{0} \\ \underline{G} \end{bmatrix} \underline{u}_{ev} = \begin{bmatrix} \underline{0} & \underline{M}^{-1}\underline{M}_d \\ -\underline{M}_d\,\underline{M}^{-1} & \underline{J}_z(\underline{q},\underline{p}) \end{bmatrix} \begin{bmatrix} \nabla_{\underline{q}} H_d \\ \nabla_{\underline{p}} H_d \end{bmatrix} \tag{7}$$

The first row is always true, whereas the second row leads to

$$\underline{G}\,\underline{u}_{ev} = \nabla_{\underline{q}} H - \underline{M}_d\,\underline{M}^{-1} \nabla_{\underline{q}} H_d + \underline{J}_z\,\underline{M}_d^{-1}\,\underline{p} \tag{8}$$

considering $\nabla_{\underline{p}} H_d = \underline{M}_d^{-1}\,\underline{p}$. The energy shifting control $\underline{u}_{ev}$ in case of an underactuated system can be stated using the left pseudo-inverse $\underline{G}^+ = (\underline{G}^T\underline{G})^{-1}\underline{G}^T$, which leads to

$$\underline{u}_{ev} = \underbrace{(\underline{G}^T\underline{G})^{-1}\underline{G}^T}_{=\underline{G}^+} \left(\nabla_{\underline{q}} H - \underline{M}_d\,\underline{M}^{-1} \nabla_{\underline{q}} H_d + \underline{J}_z\,\underline{M}_d^{-1}\,\underline{p}\right) \tag{9}$$

Introducing the orthogonal vektor $\underline{G}^{\perp}$ according to $\underline{G}^{\perp}\underline{G} = 0$, the control law $\underline{u}_{ev}$ must be subject to:

$$\underline{G}^{\perp}\left[\nabla_{\underline{q}} H - \underline{M}_d\, \underline{M}^{-1} \nabla_{\underline{q}} H_d + \underline{J}_z\, \underline{M}_d^{-1}\, \underline{p}\right] \stackrel{!}{=} 0 \tag{10}$$

This problem can be devided in two parts. A first equation that is independent on the momentum vector $\underline{p}$, and a second equation that depends on this momentum vector $\underline{p}$. This results in two partial differential equations that allow for calculating the closed-loop mass matrix $\underline{M}_d$ and the additional interconnection matrix $\underline{J}_z$.

$$\underline{G}^{\perp}\left[\nabla_{\underline{q}} V - \underline{M}_d\, \underline{M}^{-1} \nabla_{\underline{q}} V_d\right] = \underline{0} \tag{11}$$

$$\underline{G}^{\perp}\left[\nabla_{\underline{q}} (\underline{p}^T \underline{M}^{-1}\, \underline{p}) - \underline{M}_d\, \underline{M}^{-1} \nabla_{\underline{q}} (\underline{p}^T \underline{M}_d^{-1}\, \underline{p}) + 2\, \underline{J}_z\, \underline{M}_d^{-1}\, \underline{p}\right] = \underline{0} \tag{12}$$

The control design is straight-forward when the mass matrix $\underline{M}$ is constant and inpendent of $\underline{q}$ ist. In this case the closed-loop a constant mass matrix $\underline{M}_d$ is used and the additional interconnection matrix $\underline{J}_z = \underline{0}$ can be chosen as zero matrix. Then the control law is obtained by evaluating (11) directly.

4 Passivity-Based Control Design for the *y*-Axis

For the passivity-based control design for the y-axis, the equations of motion are employed with the vector of generalized coordinates $\underline{q} = [y_k,\ \varphi_y]^T$. For the input vector $\underline{G}$, an orthogonal vector $\underline{G}^{\perp}$ has to be determined such that $\underline{G}^{\perp}\underline{G} = 0$ holds. In the given case the required vector is $\underline{G}^{\perp} = [0,\ 1]$. At the control design, the desired energy function in terms of the sum of kinetic and potential energy has to be specified such that a global minimum is obtained in the desired equilibrium point $\underline{q}^* = [y_{k,d},\ 0]^T$. In order to simplify the controller design, the mass matrix $\underline{M}$ is linearized for small rope angles q_2: $\cos(q_2) \approx 1$. The resulting mass matrix becomes

$$\underline{M}_{lin} = \begin{bmatrix} m_l + m_k & m_l\, l_s \\ m_l\, l_s & m_l\, l_s^2 \end{bmatrix}, \tag{13}$$

which is independent of the generalized coordinates q_1 and q_2. Therefore, the symmetric mass matrix of the closed-loop $\underline{M}_d$ can be chosen as

$$\underline{M}_d = \begin{bmatrix} a_1 & a_2 \\ a_2 & a_3 \end{bmatrix} \tag{14}$$

The elements a_1,a_2 und a_3 of the mass matrix $\underline{M}_d$ are, according to the linearized mass matrix $\underline{M}_{lin}$, independent of the vector of generalised coordinates $\underline{q}$. To obtain an asymptotically stable closed-loop system, the new mass matrix $\underline{M}_d$ must be chosen positive definite. As a result, the following conditions for the elements of $\underline{M}_d$

can be stated: $a_1 > 0$ and $a_1\, a_3 > a_2^2$. Now, the potential energy of the closed-loop system V_d can be specified using (11) with $\underline{\underline{M}} = \underline{\underline{M}}_{lin}$.

$$\left(\frac{a_2}{m_k} - \frac{a_3}{l_s\, m_k}\right) \frac{\partial\, V_d}{\partial q_1} + \left(\frac{a_3\ (m_l + m_k)}{{l_s}^2\, m_l\, m_k} - \frac{a_2}{l_s\, m_k}\right) \frac{\partial\, V_d}{\partial q_2} = m_l\, g\, l_s\ \sin(q_2) \quad (15)$$

This partial differential equation for $V_d(q_1, q_2)$ equation can be solved using computer algebra packages like *Maple*. The following solution is obtained:

$$\begin{aligned} V_d &= \frac{{m_l}^2\, g\, {l_s}^3\, m_k\ \cos(q_2)}{a_2\, m_l\, l_s - a_3\ (m_l + m_k)} + \Gamma \\ \text{with} \quad \Gamma &= f\,(q_2 + q_1\, \gamma) \quad \text{and} \quad \gamma = \frac{a_3\ (m_k + m_l) - a_2\, m_l\, l_s}{l_s\, m_l\ (a_3 - a_2\, l_s)} \end{aligned} \quad (16)$$

Here, Γ represents a freely selectable energy function. This energy function Γ must chosen properly such that V_d has a global minimum in the desired equilibrium point $\underline{q}^*$. Therefore, the gradient vector as well as the Hessian of the potential energy function V_d are considered. The gradient becomes

$$\nabla_{\underline{q}}\, V_d\Big|_{\underline{q}=\underline{q}^*} = \left[\begin{array}{c} \dfrac{\partial \Gamma}{\partial q_1} \\ -\dfrac{{m_l}^2\, g\, {l_s}^3\, m_k\ \sin(q_2)}{a_2\, m_l\, l_s - a_3\ (m_l + m_k)} + \dfrac{\partial \Gamma}{\partial q_2} \end{array}\right]\Bigg|_{\underline{q}=\underline{q}^*} = \left[\begin{array}{c} \dfrac{\partial \Gamma}{\partial q_1}\Big|_{\underline{q}=\underline{q}^*} \\ \dfrac{\partial \Gamma}{\partial q_2}\Big|_{\underline{q}=\underline{q}^*} \end{array}\right] \stackrel{!}{=} \underline{0} \quad (17)$$

For the desired equilibrium point $\underline{q}^*$ the gradient of the freely selectable function $\nabla_q \Gamma$ at $\underline{q}^*$ must vanish. In addition, the Hessian is considered as sufficient condition for a minimum

$$\nabla_{\underline{q}}^2\, V_d\Big|_{\underline{q}=\underline{q}^*} = \left[\begin{array}{cc} \dfrac{\partial^2 \Gamma}{\partial q_1^2} & \dfrac{\partial^2 \Gamma}{\partial q_1\, \partial q_2} \\ \dfrac{\partial^2 \Gamma}{\partial q_1\, \partial q_2} & -\dfrac{{m_l}^2\, g\, {l_s}^3 m_k\ \cos(q_2)}{a_2\, m_l\, l_s - a_3\ (m_l + m_k)} + \dfrac{\partial^2 \Gamma}{\partial q_2^2} \end{array}\right]\Bigg|_{\underline{q}=\underline{q}^*} \stackrel{!}{>} 0 \quad (18)$$

For simplicity a quadratic function Γ of the form

$$\Gamma = \frac{K}{2}\,(\tilde{q}_2 + \tilde{q}_1\, \gamma)^2 \quad (19)$$

has been chosen, where K denotes a proportional gain. The variable $\tilde{q}_1 = y_k - y_{k,d}$ stands for the tracking error in terms of the difference between the trolley position y_k and the desired trolley position $y_{k,d}$. Accordingly, the tracking error $\tilde{q}_2 = \varphi_y - \varphi_{y,d}$ represents the deviation of the measured rope angle φ_y and the desired rope angle $\varphi_{y,d}$. By evaluating the gradient vector, the following conditions are obtained:

$$\nabla_{\underline{x}} V_d = \begin{bmatrix} K\ (\tilde{q}_2 + \tilde{q}_1\,\gamma)|_{\underline{q}=\underline{q}^*} \\ K\ (\tilde{q}_2 + \tilde{q}_1)|_{\underline{q}=\underline{q}^*} \end{bmatrix} = \begin{bmatrix} 0 \\ 0 \end{bmatrix} \tag{20}$$

Next, the Hessian is investigated. This leads to

$$\nabla^2_{\underline{x}} V_d = \begin{bmatrix} K\,\gamma^2 & K\,\gamma \\ K\,\gamma & K - \dfrac{m_l^2\, m_k\, g\, l_s^3 \cos(q_2)}{a_2\, m_l\, l_s - a_3\ (m_l + m_k)} \end{bmatrix}\Bigg|_{\underline{x}^*} \tag{21}$$

The first north-western subdeterminant is positiv for $K > 0$ and $\gamma > 0$. Considering $|q_2| < pi/2$, the determinant of the Hessian is positive definite only for:

$$-\frac{K\gamma^2 {m_l}^2\, g\, {l_s}^3 m_k}{a_2\, m_l\, l_s - a_3\,(m_l + m_k)} > 0$$

The nominator is always positive; hence, the denominator must be negative in order to meet the necessary condition. This leads to an additional condition for the choice of the free design parameters a_2 and a_3: $a_3\,(m_l + m_k) > a_2\, m_l\, l_s$. The following choice has been made: $a_3 = c\, l_{\max}$, $a_1 = c/l_{\max}$ and $a_2 = m$, with the two constants c and m. These constants are selected such that $c > m > 0$ holds. The maximum rope length is given by the value $l_{\max}$. Hence, all the conditions above are fulfilled. With the energy function V_d determined, the control law can be calculated. The nonlinear control action $u_{PBC} = u_{ev} + u_{di}$ consists of the sum of the energy shifting term u_{ev} and the damping injection term u_{di}. The energy shifting is achieved by the control part u_{ev} according to

$$u_{ev} = (\underline{G}^T\,\underline{G})^{-1}\,\underline{G}^T\left(\nabla_{\underline{q}}\, V - \underline{M}_d\,\underline{M}_{lin}^{-1}\,\nabla_{\underline{q}}\, V_d\right) = K\gamma(\tilde{q}_2 + \gamma\,\tilde{q}_1)\left(\frac{a_2}{l_s\, m_k} - \frac{a_1}{m_k}\right) + \left(\frac{a_1}{l_s\, m_k} - \frac{a_2\ (m_l + m_k)}{m_l\, {l_s}^2 m_k}\right)\left(K\,(\tilde{q}_2 + \gamma\,\tilde{q}_1) - \frac{{m_l}^2 g {l_s}^3 m_k\ \sin(q_2)}{a_2\, m_l\, l_s - a_3\ (m_l + m_k)}\right) \tag{22}$$

With the constant damping gain $K_d > 0$, the damping injection control can be calculated from (6)

$$u_{di} = -K_d\left(\frac{((m_l + m_k)\,\dot{q}_1 + m_l\, l_s\,\dot{q}_2)\, a_3}{a_1\, a_3 - {a_2}^2} - \frac{\left(m_l\, l_s\,\dot{q}_1 + m_l\, {l_s}^2 \dot{q}_2\right) a_2}{a_1\, a_3 - {a_2}^2}\right) \tag{23}$$

5 Implementation of the Crane Control

In addition to the passivity-based control u_{PBC}, some structural extension have turned out to be useful at implementation to improve trajectory tracking (Figure 2).

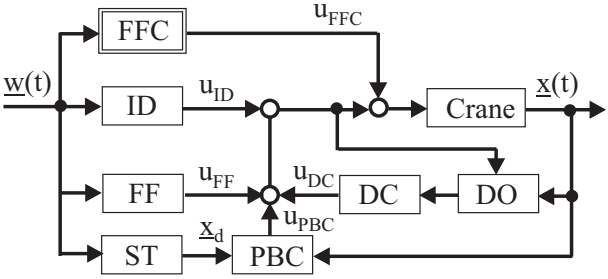

Fig. 2 Control implementation.

Hence, the stabilizing PBC is extended with feedforward control action based on an inverse system model. This feedforward control involves the following parts:

1. inverse dynamics control action u_{ID} based on the equation of motion without disturbance forces
2. feedforward compensation u_{FFC} of nonlinear friction and damping forces as main disturbances
3. a feedforward control action u_{FF} corresponding to the feedback control part u_{PBC}

The latter part u_{FF} is necessary to compensate for the feedback control in the ideal case if the design model matches the real system exactly. Then, the first two feedforward parts $u_{FFC}+u_{FF}$ would lead to a perfect trajectory tracking. In the given case of an imperfect system model with remaining uncertainties and disturbances, however, additional feedback control is mandatory. A trajectory planning module yields the desired values $\underline{w}$ for the crane load position $y_{l,d}$ as well as the corresponding first three time derivatives. For the feedforward control, however, the corresponding desired values for the trolley positions $y_{k,d}$ as well as the rope angle $\varphi_{y,d}$ and their time derivatives are required. As the system under consideration is differentially flat with the crane load position as flat control output, all the desired state variables and the control input can be calculated. In the implementation, the following linearized relationships have been used in the state transformation ST:

$$y_{k,d} = y_{l,d} + \frac{l_s}{g}\ddot{y}_{l,d}, \quad \dot{y}_{k,d} = \dot{y}_{l,d} + \frac{l_s}{g}\dddot{y}_{l,d}, \quad \varphi_{y,d} = -\frac{\ddot{x}_{l,d}}{g}, \quad \dot{\varphi}_{y,d} = -\frac{\dddot{x}_{l,d}}{g}. \tag{24}$$

With the control structure described above, sufficiently small control errors could be achieved. Nevertheless, the implemented model-based friction compensation can be significantly improved by an additional reduced order disturbance observer DO as well as an disturbance compensation DC as described in [1]. The complete control structure is adapted to the varying system parameters load mass m_l and rope length l_s by gain-scheduling.

6 Control of the x-Axis

The designed passivity-based control for the y-axis shall be used for the x-axis control as well. The crane bridge, however, is equipped with two electric drives, which have to be properly actuated to achieve both the desired motion in x-direction but also a vanishing position difference of both bridge sides. Due to an excentric trolley position on the bridge and different friction forces acting on the corresponding drives, an active synchronization of both bridge drives have to be provided instead of a simple division of the according passivity-based control action u_{PBC} in the form $u_{b,l} = u_{b,r} = 0.5 \cdot u_{PBC}$. The active synchronization is achieved by an underlying PD-control loop of high bandwidth, i.e. $m_\varphi = -K_{p,GLR}\,\varphi_{xb} - K_{d,GLR}\,\dot{\varphi}_{xb}$. The required force distribution can be derived from the following system of equations:

$$\begin{bmatrix} u_{PBC} \\ m_\varphi \end{bmatrix} = \begin{bmatrix} 1 & 1 \\ -\dfrac{l_{br}}{2} & \dfrac{l_{br}}{2} \end{bmatrix} \begin{bmatrix} u_{b,r} \\ u_{b,l} \end{bmatrix} \Leftrightarrow \quad \begin{bmatrix} u_{b,r} \\ u_{b,l} \end{bmatrix} = \begin{bmatrix} \dfrac{1}{2} & -\dfrac{1}{l_{br}} \\ \dfrac{1}{2} & \dfrac{1}{l_{br}} \end{bmatrix} \begin{bmatrix} u_{PBC} \\ m_\varphi \end{bmatrix} \tag{25}$$

Thereby, the control design for the y-axis can be used for the bridge position control as well. The x-position of the trolley depends on the y-position on the bridge and on the two position coordinates of the bridge, i.e. $x_{b,r}$ und $x_{b,l}$. This position can be calculated as follows:

$$x_k = x_{b,r} + \left(x_{b,l} - x_{b,r}\right)\left(\frac{1}{2} + \frac{y_k}{l_{br}}\right) \tag{26}$$

Consequently, by replacing the trolley mass m_k with the bridge mass m_b in (22) and (23), the resulting drive force $u_{PBC} = u_{ev} + u_{di}$ of the outer control loop in x-direction can be calculated.

7 Experimental Results

Tracking performance as well as steady-state accuracy w.r.t. the crane load position have been investigated by experiments with a 5 t-overhead travelling crane. The resulting tracking performance as regards desired trajectories in the xyz-workspace involving variations in rope length is shown in Figure 3.

8 Conclusions

This paper presents a gain-scheduled passivity-based control design for the translational axes of a 5 t-overhead travelling crane. The feedback control is extended by

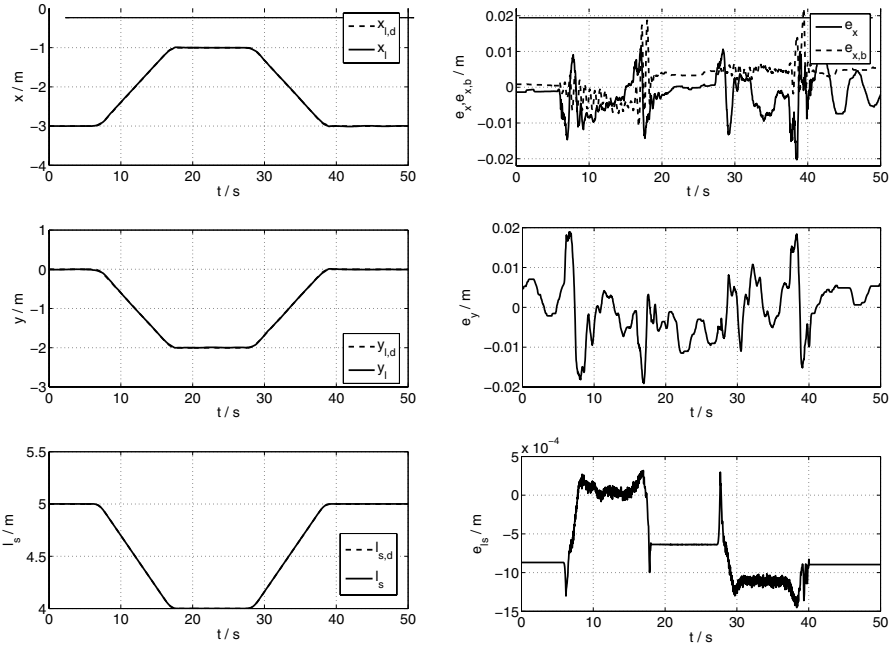

Fig. 3 Synchronised movement in the xyz-workspace with varying rope length.

feedforward control exploiting the differential flatness of the system. Furthermore, a reduced-order disturbance observer takes into account the remaining model uncertainties due to nonlinear friction acting on the trolley. The efficiency of the proposed control is shown by experimental results involving tracking of desired trajectories within the 3-dimensional workspace. Maximum tracking errors are approx. 2 cm.

References

1. Aschemann, H.: *Optimale Trajektorienplanung sowie modellgestütze Steuerung und Regelung für einen Brückenkran*. Fortschrittberichte VDI, Reihe 8, Nr. 929, VDI Verlag, Düsseldorf (2002).
2. Boustany, F., d'Andrea-Novel, B.: Adaptive Control of an Overhead Crane Using Dynamic Feedback Linearization and Estimation Design. In: *Proc. IEEE Int. Conf. on Robotics and Automation*, Nice, France, pp. 1963–1968 (1992).
3. Janzen, A.: Passivitätsbasierte Regelung mechatronischer Systeme. Diploma thesis, University of Ulm, Germany (2006).
4. Lozano, R., Brogliato, B., Egeland, O., and Maschke, B.: *Dissipative Systems Analysis and Control: Theory and Applications*. Springer (2000).
5. Nguyen, H.T.: State Variable Feedback Controller for an Overhead Crane. *J. Electr. Electr. Eng.* **14**(2), 75–84 (1994).
6. Rodriguez, H., Ortega, R., and Mareels, I.: A Novel Passivity-Based Controller for an Active Magnetic Bearing Benchmark Experiment. In: *Proc. of the ACC 2000*, Chicago, Illinois (2000).
7. van der Schaft, A.: *L_2-Gain and Passivity Techniques in Nonlinear Control*. Springer (2000).